

Estimation of Utility-Maximizing Bounds on Potential Outcomes

Maggie Makar
CSAIL, MIT
mmakar@mit.edu

Fredrik D. Johansson
Chalmers University of Technology
fredrik.johansson@chalmers.se

John V. Guttag
CSAIL, MIT
gutttag@mit.edu

David Sontag
CSAIL, MIT
dsontag@mit.edu

Abstract

Estimation of individual treatment effects is often used as the basis for contextual decision making in fields such as healthcare, education, and economics. However, in many real-world applications it is sufficient for the decision maker to have upper and lower bounds on the potential outcomes of decision alternatives, allowing them to evaluate the trade-off between benefit and risk. With this in mind, we develop an algorithm for directly learning upper and lower bounds on the potential outcomes under treatment and non-treatment. Our theoretical analysis highlights a trade-off between the complexity of the learning task and the confidence with which the resulting bounds cover the true potential outcomes; the more confident we wish to be, the more complex the learning task is. We suggest a novel algorithm that maximizes a utility function while maintaining valid potential outcome bounds. We illustrate different properties of our algorithm, and highlight how it can be used to guide decision making using two semi-simulated datasets.

1 Introduction

In many practical situations, upper and lower bounds of the causal effect of an intervention are sufficient to inform decision making. For example, knowing that heparin, an anticoagulation medication, decreases the patient’s risk of a stroke by 5–10%, in most cases, is just as useful as knowing that it decreases that risk by 7.23%. In addition, estimates of the potential outcomes resulting from alternative choices of treatment are sometimes more useful than the difference between the two, referred to as the Individual Treatment Effect (ITE). For example, learning that heparin decreases the patient’s risk of stroke from 30 to 10% rather than 60 to 40% might lead her to overlook the inconvenience of some side effects, and opt to take the treatment. For these reasons, we consider the task of estimating high-confidence covariate-conditional bounds on potential outcomes using observational data.

Most existing methods for estimating causal effects and potential outcomes attempt to fit the expected outcomes as functions of observed covariates, relying on variants of Empirical Risk Minimization (ERM) strategies [10, 22, 1, 2]. Some of these methods produce prediction intervals centered around the estimated expected response surface, which can be used to

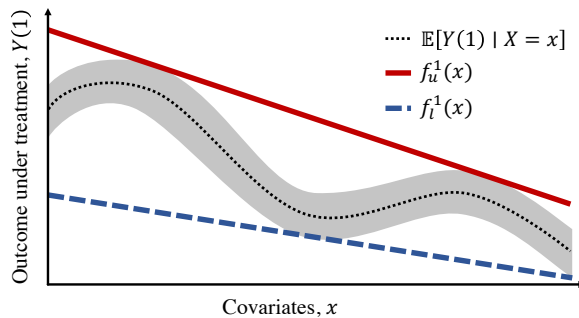


Figure 1: Illustration of the intuition behind our theoretical findings. While the true potential outcome (black/gray) belongs to a complex class, the upper (red) and lower (blue) bounds f_u^1, f_l^1 that correctly cover it belong to a simple linear function space.

bound the response from above and below. These intervals have approximately valid coverage for large samples, provided that the mean estimate is sufficiently unbiased. However, this is not always feasible in small samples, leading to high false coverage rates (FCRs), defined as the rate at which samples are observed outside of the given prediction interval.

Instead of attempting to fit the full response surfaces, which may be complex and hard to estimate accurately from small samples, we propose to fit simpler functions that bound the outcome from above and below. Within this constrained function class, we identify estimates of the potential outcomes that maximize a specific utility function specified by the decision maker. Figure 1 shows the intuition behind our approach. For example, we might wish to find estimates that give us the most certainty in the true potential outcomes on average (i.e., the tightest bounds in expectation), or the ones that maximize the worst-case utility, (e.g., minimize the maximum interval width).

We make the following main contributions: (i) We give results on the generalization properties of learned bounds on potential outcomes and the conditions under which estimation of such bounds yields better sample complexity than fitting the expected outcomes using standard risk minimization methods. Our analysis highlights a trade-off between confidence that the bounds correctly cover the data and the complexity of the learning task. (ii) We design an algorithm that searches within a constrained function family to find the function that maximizes a given utility function while providing high-confidence bounds. We explore different utility functions, analyzing the differences between the resulting bounds, and prove equivalence to quantile regression in a special case. (iii) We evaluate our algorithm on several semi-synthetic datasets and show how it can guide treatment decisions, and that it achieves a better trade-off between bound violations and utility than baseline algorithms.

2 Related work

Research into methods for estimating conditional causal effects have focused primarily on estimating the full expected potential outcomes or conditional average treatment effect (CATE) as functions of the observed covariates [9], and the same is true of theoretical work. For example, Alaa and van der Schaar [1] showed that the CATE estimation problem is as hard as modelling the more complex of the two potential outcome surfaces in the minimax sense. Similarly, Nie and Wager [19] show asymptotic bounds that rely on the complexity of

the underlying function class of the CATE. More generally, recent work in CATE estimation has focused on the learning challenges associated with the difference between the treated and control populations, and on improving finite sample efficiency by sharing data between treatment groups [14, 22, 2, 10]. In contrast, we aim to improve sample efficiency by only providing bounds on the causal estimands.

Other work focuses on estimating lower or upper bounds of Average Treatment Effect (ATE), to account for the possibility of unobserved confounding [3, 4, 20, 5]. Recently, this type of analysis was extended to include bounds on CATE, but again in the presence of hidden confounding [15]. This line of work falls under sensitivity analysis, which is distinct from our work in that we aim to find bounds on the potential outcomes even in the absence of unobserved confounding.

Another related line of work is the problem of conditional quantile treatment effect estimation [16, 6]. The similarity lies in that both our method and quantile methods give bounds on the potential outcomes. The distinction is that the main objective of our method is not to estimate the specific quantile of treatment effect, but rather to provide the simplest functions that bound the outcomes such that a specific utility is optimized; we do not wish in general to establish asymptotic convergence to a particular quantile of the treatment effect. However, as we prove later, quantile estimation is a special case of our setting for a certain utility function.

Our work is related to offline policy learning. For example, Swaminathan and Joachims [26, 25], Joachims et al. [13] address the issue of “risky” policies by explicitly picking ones with small variance rather than just optimizing for the reward. The main difference between this work and ours is that we wish to obtain bounds for the potential outcomes, not just the value of the optimal policy. This allows the user to consider the estimated effect of the treatment against a backdrop of additional information that may not be recorded in the observational data.

3 Background

We consider learning of bounds on potential outcomes from finite-sample observational data, adopting the notation of the Neyman-Rubin potential outcomes framework [21]. For each unit i (e.g. patient), we observe a set of features $X_i \in \mathcal{X}$, with \mathcal{X} a bounded subset of \mathbb{R}^d , an action (also known as treatment or intervention) $T_i \in \{0, 1\}$ and an outcome $Y_i \in \mathbb{R}$. We observe these variables through samples $(x_1, t_1, y_1), \dots, (x_n, t_n, y_n) \stackrel{i.i.d.}{\sim} p(X, T, Y)$ and denote by $n_t = \sum_{i=1}^n \mathbb{1}[t_i = t]$ the number of observed samples for treatment group $t \in \{0, 1\}$, and let $p_t(X) = p(X | T = t)$. The observed outcome is one of the two *potential outcomes*, $Y(0)$ and $Y(1)$, under control ($T = 0$) and treatment ($T = 1$), respectively.

We seek to learn high-probability bounds on both potential outcomes, $Y(0)$ and $Y(1)$, conditioned on the set of observed features X . Since only one outcome is observed, the other is not identifiable without strong assumptions. To that end, we assume that the features X are sufficient to deconfound estimates of $Y(0), Y(1)$:

Assumption 1. *The features X , treatment T and potential outcomes $Y(0), Y(1)$ satisfy for some $\epsilon > 0$*

1. *Strong ignorability: $Y(0), Y(1) \perp\!\!\!\perp T | X$*

2. *Overlap*: $\forall x, t : p(T = t | x) > \epsilon$
3. *Consistency*: $Y = Y(T)$

Under Assumption 1, $p(Y(t) = y | X = x) = p(Y = y | T = t, X = x)$ [11]. This means that the distribution of potential outcomes may be estimated through regression or other standard methods. When treatment and outcomes are confounded, i.e., Assumption 1 holds only for $X \neq \emptyset$, averages over the sub-population $p(X | T = t)$ are biased estimates of the expectation over $p(X)$. For example, if medication A was prescribed more often to terminally ill patients than the alternative treatment B, we might learn that the life expectancy on treatment A was lower than on B, regardless of its average causal effect. To undo this bias, it is common to use the propensity score $e(x, t) := p(T = t | X = x)$ to re-weight the cohort using importance weighting.

Definition 1. *The importance weighting function w_t for group $t \in \{0, 1\}$ is $w_t(x) := p(T = t)/e(x, t)$.*

We use w_i to denote $w_{t_i}(x_i)$ for a sample $(x_i, t_i) \sim p$. With w_t as in Definition 1, we have for an arbitrary function f on \mathcal{X} (e.g., the expected outcome or a prediction loss), $\mathbb{E}_X[f(X)] = \mathbb{E}_{X|T}[w_t(X)f(X) | T = t]$.

4 Generalization of bounds on potential outcomes

Our goal is to estimate four functions; lower and upper bounds for the potential outcome under treatment, $\mathbf{f}^1(x) = \{f_l^1(x), f_u^1(x)\}$, and similarly defined functions for the outcome under control $\mathbf{f}^0(x) = \{f_l^0(x), f_u^0(x)\}$. For these estimates to be useful for decision-making, we want to make the assertion that for some small $\delta' > 0$, and for $t \in \{0, 1\}$, we have false coverage rate (FCR) bounded by δ' ,

$$\text{FCR}_{\mathbf{f}^t} := \Pr_{X, Y(t)} \left[Y(t) \notin [f_l^t(X), f_u^t(X)] \right] \leq \delta' . \quad (1)$$

Here, we note that $p(X, Y(t)) \neq p(X, Y | T = t)$, due to confounding—we want high-probability bounds over the full population $p(X)$. Moreover, in general, there may not be finite functions f_l, f_u such that this holds for $\delta' = 0$, such as when Y is Normal distributed.

Without loss of generality, we will focus on estimating a lower bound for the outcome under treatment, meaning we will focus on finding some $f_l^1(x)$ such that for a small $\delta > 0$, we have that

$$\Pr_{X, Y(t)} [f_l^1(X) \leq Y(1)] \geq 1 - \delta. \quad (2)$$

It will be useful to restate our objective in terms of the (signed) residual of a function f , defined next.

Definition 2. *For an arbitrary function f , the signed residuals for $x, y \in \mathcal{X} \times \mathcal{Y}$: $r_f(x, y) = y - f(x)$.*

Expression (2) can be restated as $\Pr[r_{f_t^1}(X, Y(1)) \geq 0] \geq 1 - \delta$. Under Assumption 1, this probability is identifiable from observed data. However, to be more cautious, we might wish to leave a “buffer zone” or a margin, and instead demand that $r_{f_t^1}(x, y) \geq \gamma$ for some $\gamma > 0$. Hence, in this setting, a violation occurs when $r_{f_t^1}(x, y) < \gamma$. Larger values of γ would imply higher confidence that we are unlikely to observe a violation of the bounds, i.e., unlikely to return an estimate of the lower bound that is greater than the true value or overestimate the outcome under treatment. With that, direct parallels could be drawn between our setup and that of maximum-margin algorithms: We want to ensure that the signed residual is larger than 0 by a margin of γ . The larger γ is, the more confident we are that our lower bound holds. We can now define the unobserved risk that we wish to study:

Definition 3. For $f_t^1 \in \mathcal{F}$, $\gamma > 0$, we define the risk of overestimation over the full unknown distribution:

$$\underline{R}_{f_t^1}(\gamma) = \mathbb{E}_{X, Y(t)} \left[\mathbb{1}\{r_{f_t^1}(X, Y(t)) < \gamma\} \right].$$

In observational studies, treatment assignment is often biased depending on patient covariates. This means that (X, Y) are drawn from a distribution that is different from the one over which we wish to estimate and minimize the risk. We deal with that by focusing on a re-weighted risk, defined as:

$$\underline{R}_{f_t^1}^w(\gamma) = \mathbb{E}_{X, Y|T} \left[w(x) \mathbb{1}\{r_{f_t^1}(X, Y) < \gamma\} \mid T = t \right]$$

Under Assumption 1, $\underline{R}_{f_t^1}(\gamma) = \underline{R}_{f_t^1}^w(\gamma)$. For the empirical error, it will be more useful to reason about the magnitude of margin violations, which is defined next.

Definition 4. For $z = \{x_i, y_i\}_{i:t_i=1}$, where $x_i, y_i \sim p_1(X, Y)$, known w_1 , $f_t^1 \in \mathcal{F}$, and $\gamma > 0$, we define the magnitude of training set violations as

$$\underline{D}^{w_1}(z, f_t^1, \gamma) = \sum_{x, y \in z} w_1(x) \min\{0, \gamma - r_{f_t^1}(x, y)\}$$

In the next section, we give bounds on expected margin violation as a function of \underline{D}^{w_1} . We rely on the covering number as a measure of complexity of the analyzed function classes, as defined in [23] and in the supplement.

4.1 Generalization of re-weighted estimators

Our main objective will be to bound the risk of overestimating $Y(1)$ over the whole distribution $p(X)$, i.e., bound $\underline{R}_{f_t^1}(\gamma)$ for an estimate f_t^1 of the lower bound on $Y(1)$. The challenge we face here is that this bound is defined with respect to $p(X)$ whereas the data are sampled from $p(X \mid T = 1)$. We will make use of sample re-weighting to address this issue. By Assumption 1, we have that the importance weights are bounded, meaning that for some $C_t < \infty$ and $t \in \{0, 1\}$:

$$\sup_{x \in \mathcal{X}} w_t(x) = \sup_{x \in \mathcal{X}} \frac{p(T = t)}{\eta_t(x)} = 2^{\mathcal{D}_\infty(p \parallel p_t)} = C_t, \quad (3)$$

where $D_k(p||q)$ is the k^{th} -order Rényi divergence. It will be convenient to denote $2^{D_k(p||q)}$ by $d_k(p||q)$. Since $2^{D_{k-1}(p||p_t)} < 2^{D_k(p||p_t)}$, we have $d_2(p||p_t) < C_t$.

Throughout, let $z_t = \{(x_i, y_i)\}_{i:t_i=t}$ denote the observed samples from treatment group t such that $x_i, y_i \sim p_t(X, Y)$. Building on the results of Cortes et al. [7], we state our first finding.

Lemma 1. *Let $\gamma > 0$ and suppose that $f_l^1 \in \mathcal{F}$ satisfies $r_{f_l^1}(x, y) \geq \gamma, \forall x, y \in z_1$. Then with probability at least $1 - \delta$, we have that,*

$$\underline{R}_{f_l^1}(\gamma) \leq \frac{4C_1(\log \mathcal{N}(\gamma, \mathcal{F}, 2n_1) + \log \frac{1}{\delta})}{3n_1} + \sqrt{\frac{8d_2(p||p_1)(\log \mathcal{N}(\gamma, \mathcal{F}, 2n_1) + \log \frac{1}{\delta})}{n_1}}.$$

The proof is given in the supplement. Lemma 1 states that if there exists a function such that all the signed residuals of the training data exceed γ then the risk with respect to the full population depends on the γ -covering number, and the discordance between the treated sample distribution and the distribution under random treatment assignment. The larger the value of the confidence parameter γ , the simpler the function class. Similar statements can be made for f_l^0, f_u^1 and f_u^0 . Next, we explore what happens if the estimated function violates the margin of γ on the training data.

Theorem 1. *Let $\gamma > 0$ and $f_l^1 \in \mathcal{F}$, where \mathcal{F} is the class of real valued functions with range $[a, b]$. Then with probability $1 - \delta$, for some k_t (defined below) that depends on $\mathcal{F}, \underline{D}^{w_1}$, and C_1 as defined in (3) we have*

$$\underline{R}_{f_l^1}(\gamma) \leq \frac{4C_1(k_1 + \log \frac{1}{\delta})}{3n_1} + \sqrt{\frac{8d_2(p||p_1)(k_1 + \log \frac{1}{\delta})}{n_1}}. \quad (4)$$

where, for $t \in \{0, 1\}$,

$$k_t = \left\lceil \log \mathcal{N}(\gamma/2, \mathcal{F}, 2n_t) + \frac{64(b-a)\underline{D}^{w_t}(z_t, f_l^t, \gamma)}{\gamma^2} + \log \left(\frac{en_t\gamma}{8\underline{D}^{w_t}(z_t, f_l^t, \gamma)} \right) \log \left(\frac{32n_t(b-a)}{\gamma^2} \right) \right\rceil.$$

Remarks. The proof is outlined in the supplement.

1. Theorem 1 states that overestimation due to generalization depends on the log covering number of \mathcal{F} as defined by the confidence parameter γ , and the ratio of γ to the violations on the training data. Requiring that we avoid overestimation with high probability, for fixed sample size, implies a larger γ , which shrinks the space of viable functions making the first term of k —the covering number—small. For larger γ , the sum of violations on the training set, \underline{D}^{w_1} is going to be small, so the second term in k is also smaller.

2. The fact that the covering number is controlled by the confidence parameter γ shows that the complexity of this learning task relies on how certain we wish to be that the lower bound is not overestimated; the more certain we wish to be, the simpler function class or larger margin we need. This is distinct from previous literature which shows that the sample complexity of risk minimization relies on the covering number of the true function class [1].

3. Theorem 1 does not suggest a specific function class, optimization algorithm or even an optimal value for γ . For example, by estimating f_l^1 by minimizing the empirical risk with

respect to the observed outcomes and shifting all our estimates down by γ , we should not expect any gains in sample efficiency and our sample complexity should reflect the complexity of learning the true $Y(1)$. The next section, suggests an algorithm that is able to leverage our finding from Theorem 1.

In the supplement, we use Theorem 1 to get a bound on the generalization error for bounds on the ITE.

5 Learning high-confidence bounds with utility

The results in Section 4 establish that the sample complexity of learning bounds on the potential outcomes depends on how confident we wish to be that the bounds hold. In applications where it is sufficient to have reliable bounds on the potential outcomes to make good decisions, this finding can be crucial. This is especially true if the potential outcomes are complex functions that are difficult to estimate accurately using small samples.

In this section, we present the Bounded Potential outcomes algorithm (BP) for learning high-utility bounds on potential outcomes under the constraint that they are violated with low probability. The algorithm is flexible in that it can be used to incorporate different objectives that the decision maker might have. BP leverages our theoretical findings by explicitly constraining estimates to satisfy a required FCR, by seeking a solution to the following problem:

$$\begin{aligned} & \underset{\mathbf{f}=\{f_u, f_l\}}{\text{maximize}} && \text{Utility}(\mathbf{f}) \\ & \text{subject to} && \text{FCR}_{\mathbf{f}} \leq \text{Required FCR}, \end{aligned}$$

with FCR defined in (1). The appropriate utility function will vary between applications. In this work, we restrict ourselves to utility functions defined in terms of the interval width (IW) of bounds $\mathbf{f} := (f_u, f_l)$

$$\text{IW}_{\mathbf{f}}(x) := f_u(x) - f_l(x) . \tag{5}$$

We consider optimizing three aggregates of IW over $p(x)$: The first (L1) represents the desire to achieve a tight prediction bound on average, captured in the mean absolute interval width. The second (L2) penalizes the mean squared interval width to place a higher penalty on points with very loose bounds. The third (L ∞) is aimed at achieving a tight bound in the worst case by considering the maximum interval width.

We consider learning under the following conditions. Define $\phi : \mathcal{X} \rightarrow \mathcal{R}$ to be a feature map such that the inner product of the image ϕ can be computed with some kernel $k(x_i, x_j) = \langle \phi(x_i), \phi(x_j) \rangle$. For treatments $t \in \{0, 1\}$ and bounds $b \in \{l, u\}$ (lower/upper), let $f_b^t(x_i) := \langle \theta_b^t, \phi(x_i) \rangle + \rho_b^t$. In this setting, all three losses (L1, L2, L ∞) are convex in θ . Let sample weights w_{t_i} be defined as in Definition 1, and define $\tilde{w}_{t_i} := w_{t_i} / \sum_{j:t_j=t_i} w_{t_j}$, for $i = 1, \dots, n$. Finally, let $\Lambda(f)$ denote a term that measures complexity of f , such as the squared norm of function parameters.

5.1 Decoupled treatment groups

First, we consider estimating bounds f_u, f_l on a single potential outcome $Y(t)$, independently of others. We measure (lack of) utility using a weighted loss $L_w(\mathbf{f})$ and desire for bounds to

be violated only with small probability over $p(x)$. As the FCR implies an integer constraint, we relax (5) to reduce computation, and constrain the hinge-loss of violations instead, as is standard with zero-one losses, as follows.

$$\begin{aligned}
& \underset{\mathbf{f}=\{f_u, f_l\}}{\text{minimize}} && L_{\tilde{w}}(\mathbf{f}) + \alpha \Lambda(\mathbf{f}) \\
& \text{subject to} && \sum_{i:t_i=t} \tilde{w}_{t_i} \max(y_i - f_u(x_i), 0) \leq \beta_u \\
& && \sum_{i:t_i=t} \tilde{w}_{t_i} \max(f_l(x_i) - y_i, 0) \leq \beta_l \\
& && f_l(x_i) \leq f_u(x_i), \forall i : t_i = t .
\end{aligned} \tag{6}$$

In our experiments, we let the loss $L_{\tilde{w}}(\mathbf{f})$ be defined by either the mean absolute interval width, $L1 = \sum_{i:t_i=t} \tilde{w}_{t_i} |IW_{\mathbf{f}}(x_i)|$, the mean squared interval width, $L2 = \sum_{i:t_i=t} \tilde{w}_{t_i} (IW_{\mathbf{f}}(x_i))^2$, or the maximum interval width, $L\infty = \sup_{i:t_i=t} (IW_{\mathbf{f}}(x_i))$.

Problem (6) can be solved separately for the two treatment groups, as is done in two-learners or the treatment variable could be added in as a feature and the two treatment groups can be jointly trained, as is done in single-learners [18]. Minimizing the mean absolute width reduces our problem to a quantile regression with non-crossing constraints [27] for some choice of quantiles q and $1 - q$.

Theorem 2. *Assume that (6) is strictly convex and has a strictly feasible solution. Then, for any fixed quantile $q \in (0.5, 1)$, there are parameters $\beta_u, \beta_l \geq 0$ such that the minimizers f_u^*, f_l^* of (6) with absolute loss and the minimizers of the quantile loss for quantiles $(q, 1 - q)$, with non-crossing constraints, are equal.*

The proof is given in the appendix.

While the imposed constraints ensure that the desired FCR is respected, the independent objective does not make use of the “unlabeled” data from the opposite treatment group. This is addressed next.

5.2 Coupled treatment groups

In the coupled problem, we make use of samples from the counterfactual treatment group in two ways. First, we apply constraints that ensure that the lower and upper bounds do not cross also for counterfactual outcomes. Second, the loss functions are defined with respect to the full marginal distribution of subjects (including counterfactual treatment assignments).

$$\begin{aligned}
& \underset{\mathbf{f}^t=\{f_u^t, f_l^t\}}{\text{minimize}} && L_{\tilde{w}}(\mathbf{f}^0, \mathbf{f}^1) + \alpha \cdot (\Lambda(\mathbf{f}^0) + \Lambda(\mathbf{f}^1)) \\
& \text{subject to} && \sum_{i:t_i=t} \tilde{w}_{t_i} \max(y_i - f_u^t(x_i), 0) \leq \beta_u, \forall t \\
& && \sum_{i:t_i=t} \tilde{w}_{t_i} \max(f_l^t(x_i) - y_i, 0) \leq \beta_l, \forall t \\
& && f_l^t(x_i) \leq f_u^t(x_i), \forall t, i : t_i = t .
\end{aligned} \tag{7}$$

We define the coupled version of the mean absolute loss $L1 = \sum_{i=1}^n \sum_{t=0}^1 \tilde{w}_{t_i} IW_{\mathbf{f}^t}(x_i)$, mean squared interval width, $L2 = \sum_{i=1}^n \sum_{t=0}^1 \tilde{w}_{t_i} IW_{\mathbf{f}^t}(x_i)^2$, and maximum interval width, $L\infty = \sup_{i=1}^n \sum_{t=0}^1 IW_{\mathbf{f}^t}(x_i)$.

Given Assumption 1, specifically, the assumption of overlap this encourages the counterfactual outcome intervals to be small even if the corresponding treatment assignment is not observed. By coupling the two objectives, we allow information to be shared between the treated and non-treated populations in a semi-supervised way. We caution, however, that in the absence of overlap, the coupled loss might be overly optimistic about in regions of non-overlap, returning intervals that do not cover the true data.

With f_l, f_u linear in the representation ϕ and $\Lambda(f)$ defined as the L2 norm of the function weights, expressions (6) and (7) are both convex programs which can be readily solved by a general purpose solver. The optimization procedure gives bounds which correspond to $\gamma = 0$, so we define an additional parameter that shifts the upper (lower) bounds by a positive (negative) value. The value of the parameter is picked based on cross-validation as discussed in the next section.

The methods presented so far leverage our theoretical findings by explicitly constraining estimates to ensure that they satisfy the required FCR. Alternatively, the function class could be implicitly restricted to functions that satisfy the required FCR by defining a two-step cross-validation procedure. First, the set of admissible hyperparameters is restricted to those which achieve the required FCR. From this restricted set, the optimal hyperparameters which maximize the utility function are picked. We refer to this method as the *restricted* method, and our main method as the *constrained* method. We compare their performance next.

6 Experiments

We evaluate our approach in a series of experiments, first highlighting key intuitions behind the method, and illustrating how it can be used to guide decision making (Section 6.2). We then evaluate our model in a more complicated, high dimensional setting used as a benchmark for causal effect estimation (Section 6.3).

6.1 Experimental setup

We compare between three families of models. First, the **constrained** models, i.e., models that explicitly place constraints on bound violations in training. This includes our main proposed model, dubbed **BP-L2 (C)**, which minimizes the coupled version of our algorithm presented in section 5.2, with the L2 objective as the objective to be minimized. We compare this to its corresponding decoupled version **BP-L2 (D)** (section 5.1). To explore the differences between utility functions (objectives), we train also versions with L1 and L_∞ objectives (**BP-L1 (D)**, **BP-L ∞ (D)**, respectively), as described in Section 5.2. We also train two quantile regressions (**QR**) [17] for quantiles η_{QR} and $1 - \eta_{QR}$ with $\eta_{QR} \in (0, 0.5)$. As noted previously, this a special case of the decoupled version of our algorithm with linear utility function (as proven in Theorem 2).

We refer to the second family of models as the **restricted** models. This includes models that implicitly restrict the function complexity based on the FCR requirement through the two-step cross-validation described in section 5. We construct the first restricted baseline by fitting a kernel regression (**KR**) to estimate the mean $\mu_t(x) := \mathbb{E}[Y(t) | X = x]$, and then shifting the outcomes by $\pm \eta_{KR} > 0$. We construct a similar baseline using a Gaussian

Processes (**GP**), where the estimated posterior over the means, $\mu_t(x)$ is shifted by $\pm \eta_{GP} \cdot \sigma_t(x)$, for $\eta_{GP} > 0$ and $\sigma_t(x)$ is the estimated posterior variance.

Third, the **unrestricted** family of models does not attempt to restrict the complexity of the functions based on the required FCR. Instead, these models are optimized to fit the observed potential outcomes as accurately as possible. Here the hyperparameters of KR and GP are picked so that the resulting model minimizes the mean squared error of the estimated potential outcomes.

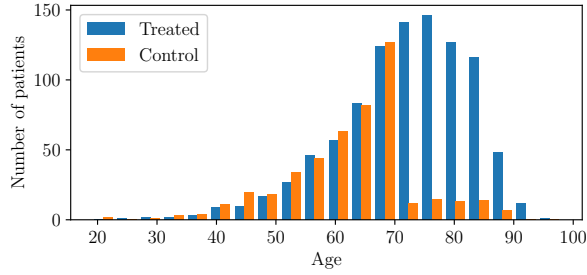
We evaluate the performance of our models and the baselines on a held-out test set with respect to two criteria: the achieved FCR, as defined in equation (1) and the utility as measured by the mean IW and the max IW, as defined in equation (5). Additional cross-validation details for our model and the baselines are included in the supplement.

6.2 IST data

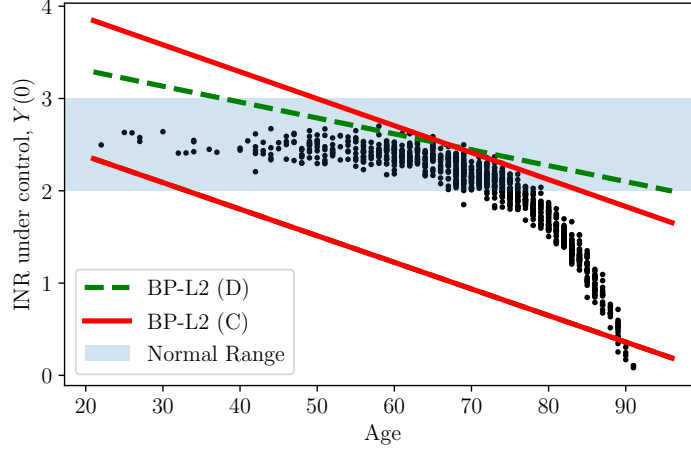
We begin with an illustrative example that highlights the strengths of our approach in a practical setting. We aim to answer the following: (1) How does the coupled objective make use of counterfactual data? (2) How do different losses reflecting different utilities of the decision maker result in different estimates?

We study the task of a physician deciding whether or not to prescribe Heparin, a medication that prevents blood clots. Patients who are at a risk of forming blood clots can reduce their risk of an Ischemic stroke by taking Heparin. Patients with healthy blood clotting mechanisms, if placed on Heparin, can experience excessive bleeding, increasing the risk of a Hemorrhagic stroke. One way to measure the patient’s ability to form clots is using the International Normalized Ratio (INR). The average healthy INR range for patients with a previous stroke is 2–3. An INR lower than 2 signals that the patient is at a higher risk of an Ischemic stroke and should take Heparin. Patients with INR higher than 3 face increased risk of a Hemorrhagic stroke if placed on Heparin. In this setting, to make an informed decision, the physician only needs to know if the outcome under treatment *roughly* falls within the healthy range; the exact value of INR does not provide additional insight.

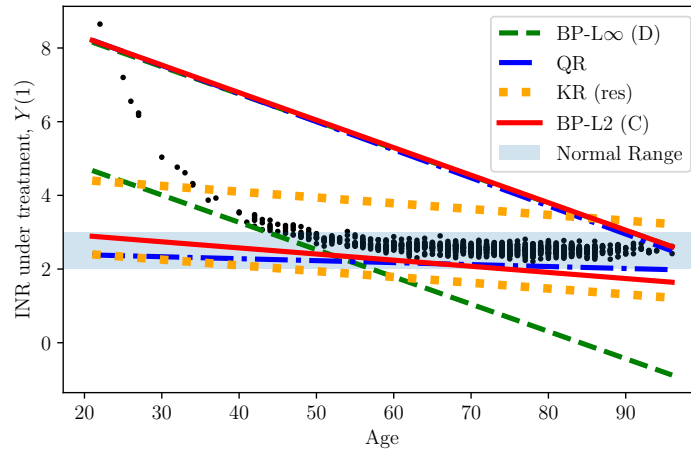
We use patient characteristics and treatment data from a randomized control trial measuring the effects of Heparin [12]. In the trial, patients were assigned to one of 4 treatment groups with equal probability; either Aspirin only, Heparin only, Aspirin and Heparin or neither. We restrict our analysis to the Heparin or neither groups, leaving us with 4530 patients on Heparin and 4534 on neither. Patient characteristics such as age, gender and disease history were measured along with some post-treatment outcomes. Because INR was not measured in the original data, we simulate the INR, under treatment according to $\mathbb{E}[Y_i(1) | age_i] \propto \exp(-0.1 \cdot age_i)$. The outcome is then re-scaled to fall within the range of 2.5–8. Similarly, the outcome under control is determined by $\mathbb{E}[Y_i(0) | age_i] \propto -\exp(0.5 \cdot age_i)$ and re-scaled to fall within the range of 0.5–3. Mean-zero Gaussian noise with variance 0.1 is added to both outcomes. The model for $Y(1)$ reflects a setting where younger patients would have too high of an INR if placed on Heparin. $Y(0)$ reflects the setting where older patients would have too low of an INR if not placed on Heparin. To introduce confounding, we drop 90% of the older (age > 70), untreated population. Note that the distribution of age in the trial is skewed, with a mean of 71.8 and a skewness of -0.79, which means that young patients are under-represented.



(a) Distribution of age in the confounded treated and control population (training).



(b) Outcome under control, $Y(0)$.



(c) Outcome under treatment, $Y(1)$.

Figure 2: Data and estimated bounds in the IST experiment. In the middle and bottom plots, black dots show potential outcomes on the test set, lines show fitted values. Middle plot shows that penalizing the counterfactual interval widths enables the coupled objective, BP-L2 (C), to return a tighter fit for $Y(0)$ in the area where few untreated examples exist in the training data (age > 70). Bottom plot shows that BP-L ∞ is a “fair” objective, ensuring that the younger (≤ 35) population has tight intervals, sacrificing tight intervals for older population. QR ensures intervals are tight for older population but returns wide intervals for the younger population. BP-L2 gives an estimate “in-between” the two objectives. KR returns bounds that are loose for older patients, and vastly underestimates the INR for patients ≤ 35 .

We assume that the physician is restricted to linear models for the purpose of interpretability, so we use a linear kernel for all the models. We randomly sample 1000 points each for training/validation and testing. For propensity scores, we fit a logistic regression. We pick the regularization parameter for the propensity score model and all the response surface models via 3-fold cross-validation as described in detail in the supplement.

Figure 2b highlights the advantage of using the coupled objective. The coupled objective returns tighter intervals for patients with age > 70 , who are under-represented in the control group. Its mean IW = 1.39, compared to that of the decoupled objective (mean IW = 1.49). This happens because the coupled objective has an incentive to minimize the interval width for old untreated patients since wider counterfactual interval for the old treated patients is penalized, whereas the decoupled objective is unaware of these patients. The estimated intervals might lead to different treatment decisions: a physician who only prescribes Heparin if both the upper and the lower bounds of the patient’s INR under non-treatment fall below the healthy range, signaling a high risk of Ischemic stroke, will rightly prescribe Heparin for patients older than 80 based on the BP-L2 (C) estimates. The loose upper bound of BP-L2 (D) for patients older than 80 (indicating INR in normal range) may lead the physician to underestimate the benefit of Heparin.

Figure 2c highlights the difference between different objectives, and how they compare to the restricted baseline. BP-L ∞ (mean IW = 3.48, max IW = 3.48) ensures that the worst-case scenario, i.e., the widest interval is always small while sacrificing the mean IW by fitting a wider interval for age ≥ 60 . Such an objective is most appropriate when issues of fairness might be at play, such as if a physician wants to ensure that younger patients are never given abnormally large intervals compared to the older group. As expected, BP-L1 performs comparably to QR; penalizing wide intervals for older patients (mean IW = 2.27, max IW = 5.76). Such an objective is appropriate when we want estimates that are as tight as possible on average, even if that entails computing wide estimates for small subpopulations. BL-L2 balances the two extremes of BP-L ∞ and BP-L1/QR; its mean IW is higher than that of BP-L1 and lower than that of BP-L ∞ (=2.40), its max IW is lower than that of BP-L1 but higher than that of BP-L ∞ (=5.26). The restricted version of KR achieves a mean and max IW = 2.00; both better than the best performing BP model. However, inspecting the fitted values reveals that (a) KR vastly underestimates the INR for ages ≤ 35 , and (b) the interval is loose for patients older than 50. A physician who prescribes Heparin only when they are certain that a patient’s INR would fall in the normal range (i.e., both upper and lower bounds fall in the normal range) would not prescribe heparin to anyone if they rely on estimates from KR or BP-L ∞ . The latter provides the advantage of correctly bounding the younger patient group, whereas the former also fails on that task.

6.3 ACIC data

Next, we evaluate our approach in a more challenging, high-dimensional task: semi-simulated data from the Atlantic Causal Inference Conference Competition [8]. In this task, 58 variables were extracted from the Collaborative Perinatal Project, a study on pregnant women and their children. The treatment assignment and the response surfaces were simulated. We focus on the simulation with limited overlap and high heterogeneity where the treatment response surface is polynomial and the response surface is exponential. We sample 200 data

Table 1: ACIC results showing performance at required FCR = 0.05 (left panel), and FCR = 0.1 (right). The unweighted version of our model, UBP-L2 (C), achieves the lowest mean interval width without violating the required FCR. Constrained and restricted models which constrain the complexity of the functions based on the required FCR outperform unrestricted model, which have the highest FCR violation.

	Req. FCR = 0.05		Req. FCR = 0.10	
	Ach. FCR	Mean IW	Ach. FCR	Mean IW
Constrained models				
BP-L2 (C)	0.06 (0.03)	32.7 (5.18)	0.12 (0.04)	25.6 (3.84)
UBP-L2 (C)	0.05 (0.01)	33.7 (4.79)	0.09 (0.02)	26.1 (3.05)
UBP-L2 (D)	0.05 (0.02)	35.1 (4.89)	0.1 (0.03)	27.4 (3.01)
QR	0.05 (0.02)	45.5 (9.47)	0.09 (0.02)	32.6 (5.0)
Restricted models				
GP (res)	0.06 (0.02)	34.8 (5.57)	0.15 (0.05)	26.4 (4.2)
KR (res)	0.04 (0.02)	38.2 (4.94)	0.09 (0.03)	29.4 (3.25)
Unrestricted models				
GP (unres)	0.27 (0.24)	22.2 (11.94)	0.33 (0.24)	17.9 (9.17)
KR (unres)	0.17 (0.13)	24.8 (7.67)	0.25 (0.14)	19.3 (5.62)

points for the training/validation set and 800 for our test set. We use an RBF kernel for all the models, and pick the bandwidth via cross-validation as outlined in the supplement. For all models, we found that the unweighted versions tend to outperform the weighted ones, so we present results from the unweighted models, UBP-L2 (C/D), and one weighted model, BP-L2. We measure the performance of the models at required FCR = { 0.05, 0.1, 0.15, 0.2 }. Due to space limitation, we present the results from required FCRs = {0.05, 0.1} in table 1, and the rest are shown in the supplement.

Table 1 shows the achieved FCR, the mean IW for our model and baselines averaged over 20 simulations. Models which achieve the lowest mean IW without violating the required FCR are in bold. Constrained and restricted models largely outperform the unrestricted models with respect to violations to the required FCR. This confirms our theoretical findings: models that restrict the complexity of the learned functions based on the required FCR perform better in finite samples. In addition, the mean IWs for all the models decrease as the FCR rate increases. This too confirms our theoretical findings that a trade-off between confidence that the bounds cover the potential outcomes and complexity of the function class; lower required FCRs (i.e., higher confidence that the bounds cover the true date) are associated with simpler function classes, which sacrifices accuracy, leading to higher mean IW. Finally, the table shows that UBP-L2 (C) outperforms baselines, achieving a lower mean IW at every FCR. While BP-L2 gives estimates with low mean IW, the variance of the achieved FCR and the mean IW is higher than that of it’s unweighted counterpart, as is typical for models that rely on inverse weighting.

7 Conclusion

In this paper we establish that the sample complexity of learning bounds on potential outcomes depends on how confident we wish to be that the bounds cover the true potential outcomes. For applications where it is sufficient to have reliable bounds on the potential outcomes to make good decisions, and the outcomes are complex functions, our findings indicate how to simplify the learning problem. Based on these findings, we introduced an algorithm that maximizes a utility function, specified by the decision maker, subject to constraints that guarantee validity of the bounds with high probability. Using semi-synthetic data, we showed that our algorithm can guide physicians in making treatment decisions for stroke patients. We also showed that our method outperforms baselines, estimating tight prediction intervals without violating a required level of false coverage rate.

Acknowledgments

We thank Uri Shalit for insightful suggestions and feedback. We thank Lucas Wittman, Amal Ramsis and Samer Moussa for medical feedback. We also thank members of the Clinical and Applied Machine Learning group at MIT. FJ was partially supported by the Wallenberg AI, Autonomous Systems and Software Program (WASP) funded by the Knut and Alice Wallenberg Foundation. MM was partially funded by Wistron Corp.

References

- [1] Ahmed Alaa and Mihaela van der Schaar. Limits of estimating heterogeneous treatment effects: Guidelines for practical algorithm design. In *Proceedings of the 35th International Conference on Machine Learning*, volume 80 of *Proceedings of Machine Learning Research*, pages 129–138. PMLR, 10–15 Jul 2018.
- [2] Ahmed M. Alaa and Mihaela van der Schaar. Bayesian inference of individualized treatment effects using multi-task gaussian processes. In *Advances in Neural Information Processing Systems 30*, pages 3424–3432. Curran Associates, Inc., 2017.
- [3] Alexander Balke and Judea Pearl. Bounds on treatment effects from studies with imperfect compliance. *Journal of the American Statistical Association*, 92(439):1171–1176, 1997.
- [4] Elias Bareinboim and Judea Pearl. Controlling selection bias in causal inference. In *Artificial Intelligence and Statistics*, pages 100–108, 2012.
- [5] Zhihong Cai, Manabu Kuroki, Judea Pearl, and Jin Tian. Bounds on direct effects in the presence of confounded intermediate variables. *Biometrics*, 64(3):695–701, 2008.
- [6] Victor Chernozhukov and Christian Hansen. An IV model of quantile treatment effects. *Econometrica*, 73(1):245–261, 2005.
- [7] Corinna Cortes, Yishay Mansour, and Mehryar Mohri. Learning bounds for importance weighting. In *Advances in Neural Information Processing Systems 23*, pages 442–450. Curran Associates, Inc., 2010.

- [8] Vincent Dorie, Jennifer Hill, Uri Shalit, Marc Scott, and Dan Cervone. Automated versus do-it-yourself methods for causal inference: Lessons learned from a data analysis competition. *arXiv preprint arXiv:1707.02641*, 2017.
- [9] Vincent Dorie, Jennifer Hill, Uri Shalit, Marc Scott, Dan Cervone, et al. Automated versus do-it-yourself methods for causal inference: Lessons learned from a data analysis competition. *Statistical Science*, 34(1):43–68, 2019.
- [10] Jennifer L Hill. Bayesian nonparametric modeling for causal inference. *Journal of Computational and Graphical Statistics*, 20(1):217–240, 2011.
- [11] Guido W Imbens and Jeffrey M Wooldridge. Recent developments in the econometrics of program evaluation. *Journal of economic literature*, 47(1):5–86, 2009.
- [12] International Stroke Trial Collaborative Group. The international stroke trial (ist): a randomised trial of aspirin, subcutaneous heparin, both, or neither among 19 435 patients with acute ischaemic stroke. *The Lancet*, 349(9065):1569–1581, 1997.
- [13] Thorsten Joachims, Adith Swaminathan, and Maarten de Rijke. Deep learning with logged bandit feedback, 2018.
- [14] Fredrik Johansson, Uri Shalit, and David Sontag. Learning representations for counterfactual inference. In *International Conference on Machine Learning*, pages 3020–3029, 2016.
- [15] Nathan Kallus, Xiaojie Mao, and Angela Zhou. Interval estimation of individual-level causal effects under unobserved confounding. *To appear in AISTATS*, 2019.
- [16] Roger Koenker and Gilbert Bassett Jr. Regression quantiles. *Econometrica: journal of the Econometric Society*, pages 33–50, 1978.
- [17] Roger Koenker and Kevin F Hallock. Quantile regression. *Journal of economic perspectives*, 15(4):143–156, 2001.
- [18] Sören R Künzel, Jasjeet S Sekhon, Peter J Bickel, and Bin Yu. Metalearners for estimating heterogeneous treatment effects using machine learning. *Proceedings of the National Academy of Sciences*, 116(10):4156–4165, 2019.
- [19] X Nie and S Wager. Quasi-oracle estimation of heterogeneous treatment effects, 2017.
- [20] Judea Pearl. *Causality*. Cambridge university press, 2009.
- [21] Donald B Rubin. Causal inference using potential outcomes. *Journal of the American Statistical Association*, 100(469):322–331, 2005.
- [22] Uri Shalit, Fredrik D Johansson, and David Sontag. Estimating individual treatment effect: generalization bounds and algorithms. In *Proceedings of the 34th International Conference on Machine Learning*, pages 3076–3085, Sydney, Australia, 2017. PMLR.
- [23] John Shawe-Taylor and Nello Cristianini. On the generalisation of soft margin algorithms. *IEEE Transactions on Information Theory*, 48(10):2721–2735, 2002.

- [24] John Shawe-Taylor and Robert C. Williamson. Generalization performance of classifiers in terms of observed covering numbers. In *Computational Learning Theory*, pages 274–285, Berlin, Heidelberg, 1999. Springer Berlin Heidelberg.
- [25] Adith Swaminathan and Thorsten Joachims. The self-normalized estimator for counterfactual learning. In C. Cortes, N. D. Lawrence, D. D. Lee, M. Sugiyama, and R. Garnett, editors, *Advances in Neural Information Processing Systems 28*, pages 3231–3239. Curran Associates, Inc., 2015.
- [26] Adith Swaminathan and Thorsten Joachims. Counterfactual risk minimization: Learning from logged bandit feedback. In *International Conference on Machine Learning*, pages 814–823, 2015.
- [27] Ichiro Takeuchi, Quoc V Le, Timothy D Sears, and Alexander J Smola. Nonparametric quantile estimation. *Journal of machine learning research*, 7(Jul):1231–1264, 2006.

8 Appendix

8.1 Generalization of lower bounds on $Y(1)$

Before stating the proof of the lemma 2 in the main paper, we introduce the following definitions and established previous results.

We define the covering number as follows:

Definition 5. Let (X, l_∞) be a pseudo-metric space defined with respect to the l_∞ norm, and let A be a subset of X and $\epsilon > 0$. A set $U \subseteq X$ is an ϵ -cover for A if for every $a \in A$, there exists $u \in U$ such that $\|a - u\|_{l_\infty} \leq \epsilon$. The ϵ -covering number of A , $\mathcal{N}(\epsilon, A, d)$ is the minimal cardinality of the ϵ -cover for A .

We define the empirical proportion overestimated as:

Definition 6. For $f \in \mathcal{F}$, $\gamma > 0$, a sample $z = \{x_i, y_i\}_i^n$ drawn from a fixed but unknown distribution p_t , known weights \mathbf{w} , we define the empirical risk when the distribution with respect to p :

$$\underline{\epsilon}_f^{\mathbf{w}}(z, \gamma) = \sum_i w(x) \mathbb{1}\{r_f(x, y) < \gamma\}.$$

Lemma 2. Due to Shawe-Taylor and Williamson [24]: Let \mathcal{F} be a sturdy function class, then for each $N \in \mathbb{N}^+$ and any fixed sequence $X \in \mathcal{X}^n$ the infimum

$$\inf\{\gamma : \mathcal{N}(\gamma, \mathcal{F}, X) < N\}$$

is attained

We assume that f_l^1, f_l^0, f_u^0 and f_u^1 belong to a sturdy function class, as defined in [24].

Definition 7. We say that a function class \mathcal{F} is sturdy if it maps X of size n to a compact subset of \mathbb{R}^n for any $n \in \mathbb{N}$.

The following lemma due to Cortes et al. [7] bounds the second moment of the weighted loss.

Lemma 3. Due to Cortes et al. [7]. For $x \in X$, a weighting function w_t on X , a loss function ℓ , and some function $f \in \mathcal{F}$, the second moment of the importance weighted loss can be bounded as follows:

$$\mathbb{E}_{X|T} \left[w_t^2(X) \ell_f^2(X) \mid T = t \right] \leq d_2(p||p_t)$$

Lemma 4 (Lemma 2 restated). Let $p_1(x) := p(x|t = 1)$, be a fixed but unknown distribution. For $z = \{x_i, y_i\}_{i=1}^{n_1}$ where $x_i, y_i \sim p_1$, and $\gamma > 0$, suppose that $f_l^1 \in \mathcal{F}$ satisfies $r_{f_l^1}(x, y) \geq \gamma$, $\forall x, y \in z$. Then with probability $1 - \delta$, we have that:

$$\underline{R}_{f_l^1}(\gamma) \leq \frac{4C_1(\log \mathcal{N}(\gamma, \mathcal{F}, 2n_1) + \log \frac{1}{\delta})}{3n_1} + \sqrt{\frac{8d_2(p||p_1)(\log \mathcal{N}(\gamma, \mathcal{F}, 2n_1) + \log \frac{1}{\delta})}{n_1}}.$$

Proof. For a given $f_l^1 \in \mathcal{F}$:

$$\begin{aligned} P\left(\underline{R}_{f_l^1}(\gamma) - \underline{\epsilon}_{f_l^1}^{\mathbf{w}}(z, \gamma) > \varepsilon\right) &= P\left(\underline{R}_{f_l^1}(\gamma) > \varepsilon\right) \\ &\leq 2P\left(\underline{\epsilon}_{f_l^1}^{\mathbf{w}'}(z', \gamma) > \frac{\varepsilon}{2}\right), \end{aligned}$$

where the equality follows from the fact that the empirical error on the estimation data will always be 0 by definition of γ . And the inequality follows from applying the double (ghost) sample trick. Suppose that such an f_l^1 exists. Pick a fixed k such that

$$\gamma_k = \inf\{\gamma : \mathcal{N}(\gamma, \mathcal{F}, 2n_1) \leq 2^k\} \leq \gamma.$$

By Lemma 2, and assumption of sturdiness, we have that this γ_k exists. Consider the γ_k -covering, U . There exists another $f_\bullet \in U$ such that the distance between f_l^1 and f_\bullet is $\leq \gamma_k \leq \gamma$, meaning f_\bullet satisfies:

$$P\left(\underline{\epsilon}_{f_l^1}^{\mathbf{w}'}(z', \gamma) > \frac{\varepsilon}{2}\right) = P\left(\underline{\epsilon}_{f_\bullet}^{\mathbf{w}'}(z', 0) > \frac{\varepsilon}{2}\right)$$

This limits the complexity of the function class from infinite to having a covering number $= C_{\mathcal{F}}^\gamma$. Swapping samples between the estimation and the ghost sample, this will create a random variable $S' = \frac{1}{M}(\underline{\epsilon}_{f_\bullet}^{\mathbf{w}'_1}(z'_1, 0) + \dots + \underline{\epsilon}_{f_\bullet}^{\mathbf{w}'_m}(z'_m, 0) + \dots + \underline{\epsilon}_{f_\bullet}^{\mathbf{w}'_M}(z'_M, 0))$ for $M = 2^{n_1}$, where the subscripts of \mathbf{w}' and z' denote the sample index. Note that $\mathbb{E}_{x \sim p_t}[S'] = \underline{R}_{f_\bullet}(0)$ and let S denote $S' - \mathbb{E}_{x \sim p_t}[S']$, with $\mathbb{E}_{x \sim p_t}[S] = 0$. Let $\sigma^2(S) = \mathbb{E}[S^2] = \mathbb{E}[(S' - \mathbb{E}_{x \sim p_t}[S'])^2]$. By Lemma 3, we have that $\sigma^2(S') \leq d_2(p||p_1) - \underline{R}_{f_\bullet}(0)^2$. By Bernstein's inequality:

$$P\left(\underline{R}_{f_\bullet}(0) - \underline{\epsilon}_{f_\bullet}^{\mathbf{w}'}(z', 0) > \frac{\varepsilon}{2}\right) \leq \exp\left(\frac{-3n_1\varepsilon^2}{24\sigma^2(S) + 4C_1\varepsilon}\right),$$

and a union bound over the function space:

$$\begin{aligned} P\left(\underline{R}_{f_\bullet}(0) - \underline{\epsilon}_{f_\bullet}^{\mathbf{w}'}(z', 0) > \frac{\varepsilon}{2}\right) &\leq \\ \mathcal{N}(\gamma, \mathcal{F}, 2n_1) \exp\left(\frac{-3n_1\varepsilon^2}{24\sigma^2(S) + 4C_1\varepsilon}\right) & \end{aligned}$$

Putting it all together:

$$\begin{aligned} P\left(\underline{R}_{f_l^1}(\gamma) - \underline{\epsilon}_{f_l^1}^{\mathbf{w}}(z, \gamma) > \varepsilon\right) &\leq 2P\left(\underline{R}_{f_\bullet}(0) - \underline{\epsilon}_{f_\bullet}^{\mathbf{w}'}(z', 0) > \frac{\varepsilon}{2}\right) \\ &\leq 2\mathcal{N}(\gamma, \mathcal{F}, 2n_1) \exp\left(\frac{-3n_1\varepsilon^2}{24\sigma^2(S) + 4C_1\varepsilon}\right) \end{aligned}$$

Setting $\delta(\varepsilon)$ to match the upper bound, inverting w.r.t. ε and removing the (negative) term $\underline{R}_{f_\bullet}(0)^2$ from the right-hand side, we get that stated bound with probability $1 - \delta$. \square

Theorem 3. (Restated theorem 1) Let $p_1(x) := p(x|t = 1)$, be a fixed but unknown distribution. For $z_1\{x_i, y_i\}_{i=1}^{n_1}$ where $x_i, y_i \sim p_1$, and $\gamma > 0$, $f_l^1 \in \mathcal{F}$, where \mathcal{F} is the class of real valued functions with range $[a, b]$. Then with probability $1 - \delta$, we have that:

$$\underline{R}_{f_l^1}(\gamma) \leq \frac{4C_1(\log k + \log \frac{1}{\delta})}{3n_1} + \sqrt{\frac{8d_2(p||p_1)(k + \log \frac{1}{\delta})}{n_1}}.$$

where

$$k = \left[\log \mathcal{N}(\gamma/2, \mathcal{F}, 2n_1) + \frac{64(b-a)\underline{D}^{w_1}(z_1, f_l^1, \gamma)}{\gamma^2} + \log \left(\frac{en_1\gamma}{8\underline{D}^{w_1}(z_1, f_l^1, \gamma)} \right) \log \left(\frac{32n_1(b-a)}{\gamma^2} \right) \right]$$

Proof. The proof relies on the auxiliary function technique outlined in [23]. It proceeds by defining an auxiliary function which is applied only on the training data. This auxiliary function serves to “shift” the points which fall outside of the margin by an amount equal to the slack. The larger the slack, the more complex the function class that this auxiliary function belongs to. The complexity of the augmented function space is shown to be bounded above by the $\log \gamma/2$ -covering number of the original function space and the covering number of the auxiliary function space. Introducing this auxiliary function allows us to easily extend lemma 2, substituting the covering number with the covering number of the augmented function space.

We next present a corollary that extends our results for lower bounding the outcome under treatment to lower bounding the ITE. A similar construction can be shown for the upper bound on the ITE. The lower bound on τ , is denoted by $\hat{\tau}_l(x)$ and is computed as $f_l^1(x) - f_0^u(x)$.

Corollary 1. Let $p_t(x) := p(x|T = t)$, be fixed but unknown distributions. For $z_t\{x_i, y_i\}_{i=1}^{n_t}$ where $x_i, y_i \sim p_t$, and $\gamma > 0$, $f_l^1, f_u^0 \in \mathcal{F}$, where \mathcal{F} is the class of real valued functions with range $[a, b]$. Let $\hat{\tau}_l = f_l^1(x) - f_0^u(x)$, then with probability $1 - \delta$, we have that:

$$\underline{R}_{\hat{\tau}_l}(\gamma) \leq \sum_t \left(\frac{4C_t(k_t + \log \frac{1}{\delta})}{3n_t} + \sqrt{\frac{8d_2(p||p_t)(k_t + \log \frac{1}{\delta})}{n_t}} \right).$$

where

$$k_t = \left[\log \mathcal{N}(\gamma/2, \mathcal{F}, 2n_t) + \frac{64(b-a)\underline{D}^{w_t}(z_t, f_t, \gamma)}{\gamma^2} + \log \left(\frac{en_t\gamma}{8\underline{D}^{w_t}(z_t, f_t, \gamma)} \right) \log \left(\frac{32n_t(b-a)}{\gamma^2} \right) \right]$$

Proof. Consider the event:

$$E = \{x : \tau(x) < \tilde{\tau}_t(x) - 4\gamma\}$$

where $x \sim p$. Note that event E implies that one of the following two events must hold:

$$E_1 = \{(x, y) : \underline{r}_{f_t^1}(x, y) < \gamma\}$$

for $t = 1$.

$$E_0 = \{(x, y_0) : \bar{r}_{f_u^0}(x, y) < \gamma\}$$

for $t = 0$.

Note that $p(E_1) = \underline{R}_{f_t^1}(\gamma)$. So, lemma 2 implies that

$$\begin{aligned} p(E_1) &\leq \frac{4C_1(\log \mathcal{N}(\gamma, \mathcal{F}, 2n_1) + \log \frac{1}{\delta})}{3n_1} \\ &+ \sqrt{\frac{8d_2(p||p_1)(\log \mathcal{N}(\gamma, \mathcal{F}, 2n_1) + \log \frac{1}{\delta})}{n_1}}. \end{aligned}$$

Similarly $p(E_0) = \bar{R}(f_u^0)$, and by a similar construction can obtain the bound on $p(E_0)$. Using a union bound we have that

$$\begin{aligned} p(E) &= p(E_1 \cup E_0) = p(E_1) + p(E_0) - p(E_1 \cap E_0) \\ &\leq p(E_1) + p(E_0), \end{aligned}$$

which completes the proof. \square

9 Equivalence to quantile regression

Consider the following problem

$$\begin{aligned} &\underset{u, l}{\text{minimize}} && \frac{1}{n} \sum_{i=1}^n L(u(x_i), l(x_i)) \\ &\text{subject to} && \frac{1}{n} \sum_{i=1}^n \max[y_i - u(x_i), 0] \leq \beta \\ &&& \frac{1}{n} \sum_{i=1}^n \max[l(x_i) - y_i, 0] \leq \beta \\ &&& u(x_i) \geq l(x_i), \quad \forall i \in [n] \end{aligned} \tag{8}$$

Theorem 4. *Assume that (8) is strictly convex and has a strictly feasible solution. Then, for any fixed quantile $t \in (0.5, 1)$, there is a parameter $\beta \geq 0$ such that the minimizer of (8) with absolute loss and the minimizer of the quantile loss, for quantiles $(t, 1 - t)$ with non-crossing constraints, are equal and have false coverage rate $1 - q$.*

Proof. Problem (8) with absolute loss $L(y, y') = |y - y'|$ can be stated as

$$\begin{aligned}
& \underset{u, l}{\text{minimize}} && \frac{1}{n} \sum_{i=1}^n (u(x_i) - l(x_i)) \\
& \text{subject to} && \frac{1}{n} \sum_{i=1}^n \max[y_i - u(x_i), 0] \leq \beta \\
& && \frac{1}{n} \sum_{i=1}^n \max[l(x_i) - y_i, 0] \leq \beta \\
& && u(x_i) \geq l(x_i), \quad \forall i \in [n]
\end{aligned}$$

Let $Q_\beta(u, l) = \frac{1}{n} \sum_{i=1}^n (u(x_i) - l(x_i))$ denote the objective and F the feasibility region. Introducing Lagrange multipliers for the first two constraints, we obtain the regularized objective

$$\begin{aligned}
L(u, l, \lambda_u, \lambda_l) &= \frac{1}{n} \sum_{i=1}^n (u(x_i) - l(x_i)) \\
&+ \frac{\lambda_u}{n} \sum_{i=1}^n \max(y_i - u(x_i), 0) - \beta \\
&+ \frac{\lambda_l}{n} \sum_{i=1}^n \max(l(x_i) - y_i, 0) - \beta
\end{aligned}$$

and by convexity and strict feasibility, strong duality holds through Slater's condition,

$$\min_{u, l \in F} Q_\beta(u, l) = \max_{\lambda_u, \lambda_l \geq 0} \min_{u \geq l} L(u, l, \lambda_u, \lambda_l) .$$

By strict convexity, for each $\beta \geq 0$, the minimizers u^*, l^* on either side are equal for the maximizers λ_u^*, λ_l^* . Now, consider the following objective, equivalent in minima to $L(\theta, \lambda_u, \lambda_l)$,

$$\begin{aligned}
\tilde{L}(\theta, \lambda_u, \lambda_l) &:= \sum_{i=1}^n (u(x_i) - l(x_i)) \\
&+ \lambda_u \sum_{i=1}^n \max(y_i - u(x_i), 0) \\
&+ \lambda_l \sum_{i=1}^n \max(l(x_i) - y_i, 0)
\end{aligned}$$

We can separate \tilde{L} into terms for which $y_i \geq u(x_i)$ and $y_i \geq l(x_i)$ respectively, adding and subtracting $\sum_i y_i$

$$\begin{aligned}
& \tilde{L}(\theta, \lambda_u, \lambda_l) \\
&= (\lambda_u - 1) \sum_{y_i \geq u(x_i)} (y_i - u(x_i)) - \sum_{y_i < u(x_i)} (y_i - u(x_i)) \\
&+ (1 - \lambda_l) \sum_{y_i \geq l(x_i)} (y_i - l(x_i)) - \sum_{y_i < l(x_i)} (y_i - l(x_i))
\end{aligned}$$

Now, let $\lambda_u = \lambda_l = 1/(1 - q)$ for $q \in (0, 1)$, which means $(1 - q) \geq 0$. Multiplying by $(1 - q)$ leaves us with

$$\begin{aligned}
& \tilde{L}(\theta, \lambda_u, \lambda_l) \\
& \propto \sum_{y_i \geq u(x_i)} q(y_i - u(x_i)) + \sum_{y_i < u(x_i)} (q - 1)(y_i - u(x_i)) \\
& + \sum_{y_i \geq u(x_i)} (1 - q)(y_i - l(x_i)) + \sum_{y_i < u(x_i)} (-q)(y_i - l(x_i)) \\
& \propto \frac{1}{n} \sum_{i=1}^n \max[q(y_i - u(x_i)), (q - 1)(y_i - u(x_i))] \\
& + \frac{1}{n} \sum_{i=1}^n \max[(1 - q)(y_i - l(x_i)), (-q)(y_i - l(x_i))] \\
& = \frac{1}{n} \sum_{i=1}^n \rho_q(y_i - u(x_i)) + \rho_{1-q}(y_i - l(x_i)),
\end{aligned}$$

where ρ_q is the quantile loss for quantile q . Recalling that our original problem had the constraint $u(x_i) \geq l(x_i)$, we recover the non-crossing constraint. The generalization to the case with sample weights follows immediately. \square

10 Generalization bound for ITE

Corollary 2. *Let $\gamma > 0$ and for $f_l^1, f_u^0 \in \mathcal{F}$, let $\tilde{\tau}_l := f_l^1 - f_u^0$. Further, let B_t denote the RHS of (4) for $k = k_t$, where k_t is defined as in Theorem 1. Then with probability $1 - \delta$, we have that $\underline{R}_{\tilde{\tau}_l}(\gamma) \leq \sum_t B_t$.*

The proof is stated in the supplement.

11 Cross-validation details

For our BP method, we have 5 hyperparameters to pick. These are α , the regularization parameter, the kernel bandwidth, β_u and β_l which are the allowed violations. The last parameter, $\eta_{BP} > 0$, is a parameter which shifts the lower bound down and the upper bound up. This parameter is needed because the solution to the optimization problem as stated in sections 5.1 and 5.2 corresponds to $\gamma = 0$. Note that the kernel bandwidth is only relevant for the experiments done on the ACIC data, but not the IST experiments since a linear kernel is used in the latter.

For the Gaussian process (GP), we pick the kernel bandwidth, the noise level added to the diagonal of the kernel. We also pick $\eta_{GP} > 0$, where the $\hat{f}_u(x_i) = \hat{\mu}_t(x_i) + \eta_{GP} \cdot \hat{\sigma}_t(x_i)$ and $\hat{f}_l^t(x_i) = \hat{\mu}_t(x_i) - \eta_{GP} \cdot \hat{\sigma}_t(x_i)$, with $\hat{\mu}_t, \hat{\sigma}_t$ being the posterior mean and variance as estimated by the GP.

For the kernel regression (KR), we pick the kernel bandwidth, and a regularization parameter the is multiplied by the L2 norm of the weights. We also pick η_{KR} where $\tilde{f}_u^{KR}(x_i) = \tilde{\mu}_t(x_i) + \eta_{KR}$ and $\tilde{f}_l^{KR}(x_i) = \tilde{\mu}_t(x_i) - \eta_{KR}$, for $\tilde{\mu}_t(x_i)$ being the predicted response value.

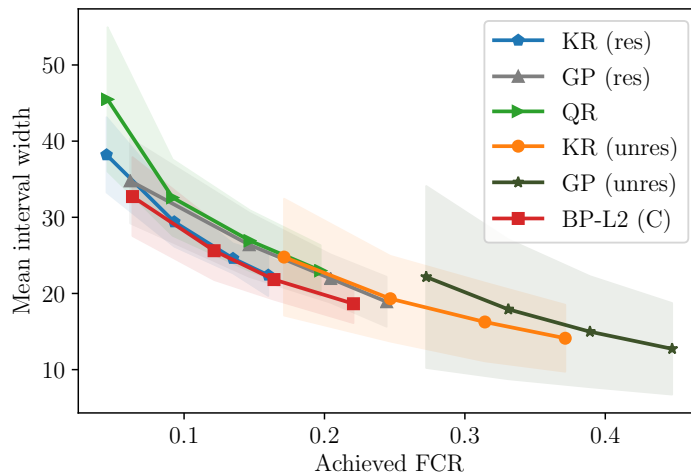


Figure 3: Achieved FCR on the x -axis, mean interval width on the y -axis. Restricted and constrained models outperform unrestricted. Lower FCRs associated with higher interval widths, highlighting the trade-off between reliable bounds (low FCRs) and complexity (more complex models are more accurate and therefore have lower mean IW)

The same applies for the GP, and KR as our BP method: the kernel bandwidth is only relevant for the experiments done on the ACIC data, but not the IST experiments since a linear kernel is used in the latter.

For the constrained methods and the restricted methods, we pick the parameters as defined in section 5: we first restrict the set of admissible hyperparameters to the ones which satisfy the required FCR and then we pick the optimal hyperparameters from this restricted set to be the ones which optimize the utility function.

For the unrestricted GP and KR, we pick the kernel bandwidths, the noise level (for the GP) and the regularization term (for the KR) to be the ones that give the lowest mean squared error on the validation set (i.e., the ones that maximize accuracy). We then pick the η_{GP} , and η_{KR} to be the ones that achieve the FCR on the held-out validation set.

12 Additional results from the ACIC experiment

Table 2 shows results for the full set of FCRs. Figure 3 is a pictorial depiction of the same results, highlighting the trade-off between FCR, and complexity.

Table 2: ACIC results showing performance at required FCR = {0.05, 0.1, 0.15, 0.2}. The unweighted version of our model, UBP-L2 (C), achieves the lowest mean interval width without violating the required FCR. Constrained and restricted models which constrain the complexity of the functions based on the required FCR outperform unrestricted model, which have the highest FCR violation.

	Req FCR = 0.05		Req FCR = 0.10		Req FCR = 0.15		Req FCR = 0.20	
	Ach. FCR	Mean IW						
Constrained								
BP-L2 (C)	0.06 (0.03)	32.7 (5.18)	0.12 (0.04)	25.6 (3.84)	0.16 (0.05)	21.8 (2.64)	0.22 (0.07)	18.7 (2.54)
UBP-L2 (C)	0.05 (0.01)	33.7 (4.79)	0.09 (0.02)	26.1 (3.05)	0.13 (0.03)	21.7 (2.29)	0.17 (0.03)	19.2 (2.15)
UBP-L2 (D)	0.05 (0.02)	35.1 (4.89)	0.1 (0.03)	27.4 (3.01)	0.14 (0.02)	23.4 (2.61)	0.2 (0.04)	20.0 (2.27)
QR	0.05 (0.02)	45.5 (9.47)	0.09 (0.02)	32.6 (5.0)	0.15 (0.04)	26.9 (4.0)	0.2 (0.04)	23.0 (3.33)
Restricted								
GP (res)	0.06 (0.02)	34.8 (5.57)	0.15 (0.05)	26.4 (4.2)	0.2 (0.05)	22.0 (3.16)	0.24 (0.05)	18.9 (3.27)
KR (res)	0.04 (0.02)	38.2 (4.94)	0.09 (0.03)	29.4 (3.25)	0.13 (0.03)	24.6 (1.96)	0.16 (0.03)	22.4 (2.72)
Unrestricted								
GP (unres)	0.27 (0.24)	22.2 (11.94)	0.33 (0.24)	17.9 (9.17)	0.39 (0.22)	15.0 (7.29)	0.45 (0.2)	12.7 (6.01)
KR (unres)	0.17 (0.13)	24.8 (7.67)	0.25 (0.14)	19.3 (5.62)	0.31 (0.15)	16.3 (5.16)	0.37 (0.15)	14.1 (4.39)